

Measurement of nuclear reaction cross sections of Li-d and Be-d at low energy

Kentaro Ochiai

Fusion Engineering Research Naka Fusion Research Establishment, JAERI

Tokai-mura, Naka-gun, Ibaraki-ken 319-11

e-mail: ochiai@fnshp.tokai.jaeri.go.jp

To estimate basic dose-rate data (PKA and KERMA) and material damage, it is important to measure nuclear cross sections of prospective candidates for blanket materials and deuteron at low energy (about 10 ~ 300 keV). And then, the nuclear reactions at low energy are also useful for Nuclear Reaction Analysis (NRA). However, we have few nuclear data of such reactions. According to we have measured nuclear-cross sections of ${}^{\text{nat}}\text{Li}(d,x)$ and ${}^9\text{Be}(d,x)$ and obtained S-factors of these reactions.

1. Introduction

Lithium and beryllium metal and these compound materials are prospective candidates for fusion plasma facing material and blanket materials. Since these materials are exposed with D-T nuclear reaction particle (3.5-MeV α and 14-MeV neutron) and plasma particles (low energy deuteron and triton) in fusion reactor, the light element of fusion-reactor materials are produced proton, deuteron, triton and helium in the material and are caused tritium activation and embitterment. Therefore, the spectroscopy analysis needs to search the material properties and especially, NRA method with low-energy deuteron beam is useful for lithium and beryllium materials. However, the spectroscopy method and these cross sections data (${}^{\text{nat}}\text{Li}(d,x)$ and ${}^9\text{Be}(d,x)$) are not enough to established such a NRA. Therefore, we have established Li-d nuclear reaction spectroscopy and obtained the cross section (and/or S-factors) of ${}^{\text{nat}}\text{Li}(d,x)$ and ${}^9\text{Be}(d,x)$,

2. Experimental procedure

The experiment was carried out using the Cockcroft-Walton type accelerator, Osaka-University, Japan and tandem-Pelletron type accelerator and Kobe University of Mercantile Marine (Fig1). Thick oxide lithium layer on backing metal (Ti) plate with LiOD-electrolysis was used as lithium sample and Beryllium sample was sheets of beryllium (10 ~ 100 μm). Two Si-SBDs with aluminum-screening foil were set up inside the vacuum chamber and the charged particles emitted from ${}^6\text{Li}(d,x)$, ${}^7\text{Li}(d,x)$ and ${}^9\text{Be}(d,x)$ reactions have been measured with the detectors (Fig.2). Since ${}^{\text{nat}}\text{Li}$ -d nuclear reactions have many kind branches, it was predicted that charged-particle spectrum emitted from Li-d reaction was piled up, therefore to separate the charged-particle spectra emitted from ${}^7\text{Li}$ -d and ${}^6\text{Li}$ -d reaction, we have used a pair of ΔE and E Si-SBD for the measurement of charged particles.

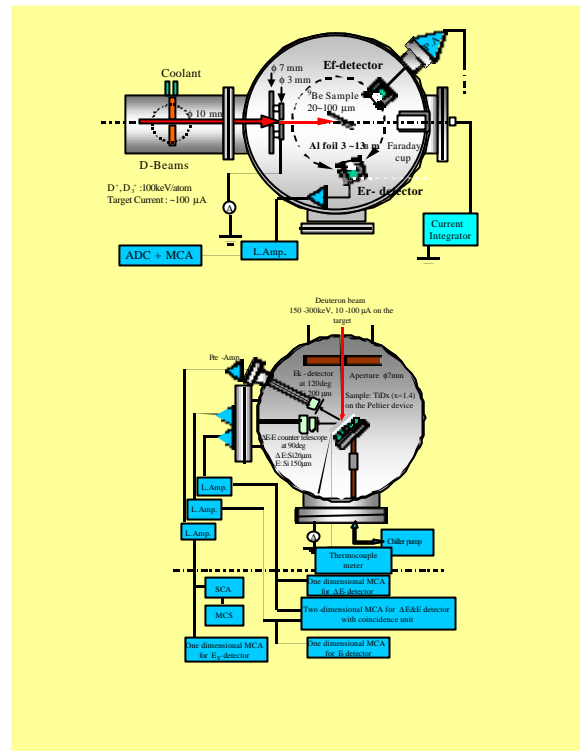
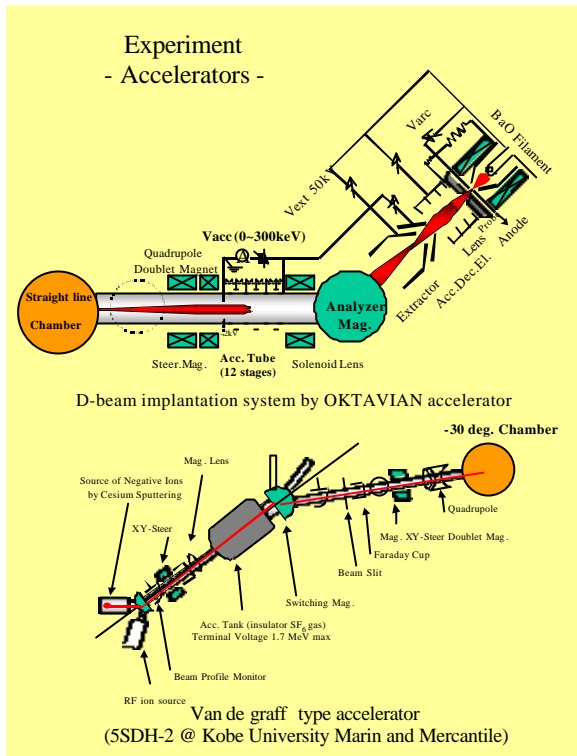


Figure 1 Apparatuses of the Cockcroft-Walton type accelerator, Osaka-University, Japan and tandem-Pelletron type accelerator and Kobe University of Mercantile Marine (left)

Figure 2 Measurement systems for the charged-particles spectroscopy of Li-d and Be-d nuclear reactions (Right)

3. Spectroscopy

Figure 3 and 4 are shown that the charged-particle spectrum emitted from Li and Be samples implanted 300-keV D^+ beam. Figure 3 is shown that 2-dimensional data of the charged-particle spectrum emitted from lithium sample implanted 300-keV D^+ beam. In case of the spectrum of $^{nat}\text{Li-d}$ reaction, measured with the ΔE and E counter method, we could have separate the charged-particle spectrum of Li-d from the charged-particle spectrum of impurity reactions ($^{12}\text{C-d}$ and D-D) have obtained clear spectrum of $^6\text{Li}(d,\alpha)$, $^7\text{Li}(d,p_0)$ and $^7\text{Li}(d,p_1)$. Figure 4 is the typical the charged-particle spectrum of $^9\text{Be-d}$ nuclear reaction. From this spectrum of detected charged particles, we have recognized the branches of $^9\text{Be-d}$ nuclear reaction. The branches which were recognized are as follow, $^9\text{Be}(d,p)$, $^9\text{Be}(d,t_0)$, $^9\text{Be}(d,t_1)$, $^9\text{Be}(d,\alpha_0)$, $^9\text{Be}(d,\alpha_1)$ and $^9\text{Be}(d,\alpha_2)$. Also the broad spectrum at ~ 2 MeV is due to ^7Li as residual particle from $^9\text{Be}(d,\alpha_0)$ and $^9\text{Be}(d,\alpha_1)$.

After we have distinguished the branches from the charged-particles spectrum, we have done the experiment to obtain the angular distributions and energy dependences of the cross sections for $^9\text{Be-d}$ nuclear reaction (at detected angle $30 \sim 150$ deg and d-beam energy $90 \sim 300$ keV).

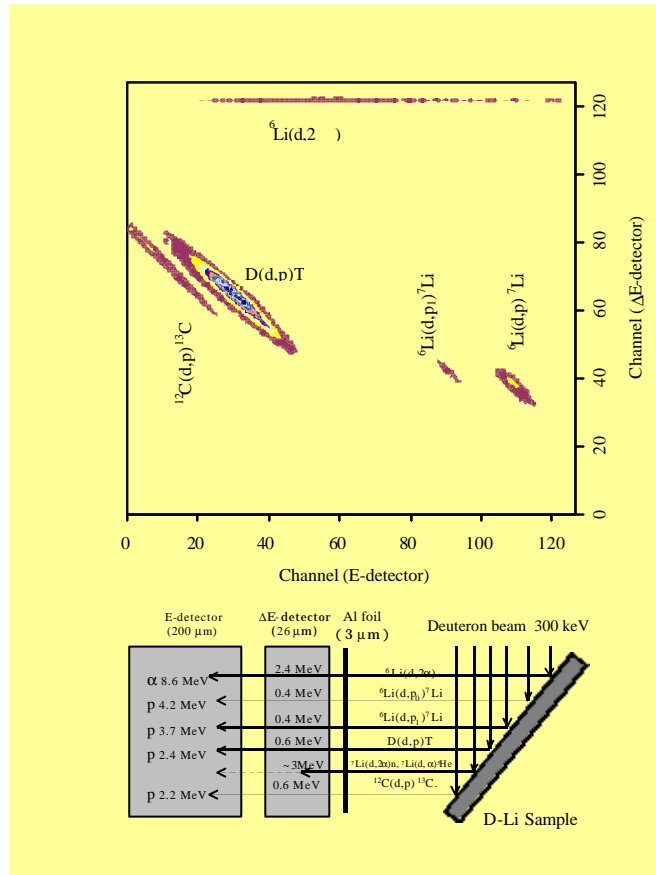


Figure 3 Contour map of the charged-particles spectrum from lithium sample using $\Delta E&E$ SSBD counter telescope

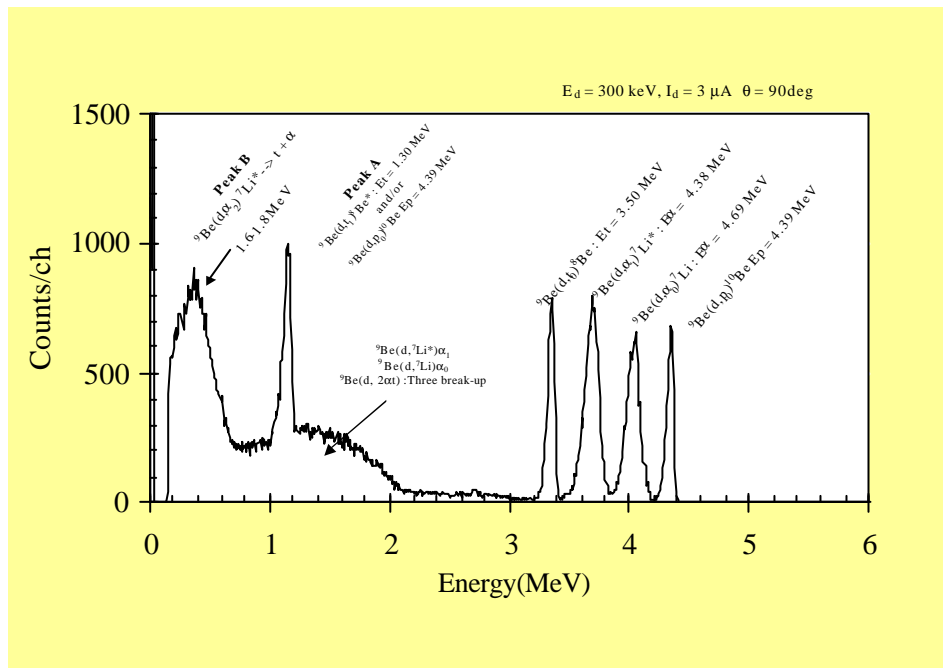


Figure 4 The typical charged spectrum from beryllium sample with 300 keV-d beam

4. Cross sections and S-factors

Figure 5 and 6 are shown that the angular distributions for ${}^9\text{Be}(d,p)$ and ${}^9\text{Be}(d,t_0)$. at $E = 280$ keV and 180 keV. The angular distributions of both cross sections tend to be backward-peaking. The differential cross sections at backward-angles for $E = 280$ keV increase about ten times at maximum larger than the value at forward-angles. The curve of the differential cross sections of ${}^9\text{Be}(d,t){}^8\text{Be}$ at $E = 280$ keV reaches a maximum value at about $\theta = 110$ degree and the differential cross section of ${}^9\text{Be}(d,t)$ at $\theta = 110$ degree is larger by two and a half times than the differential cross section at $\theta = 20$ degree. Figure 7 shows the angular distributions of differential cross sections of ${}^9\text{Be}(d,\alpha_0){}^7\text{Li}$ and ${}^9\text{Be}(d,\alpha_1){}^7\text{Li}^*$ at $E = 280$ keV. Though in Figure 7 the differential cross sections of ${}^9\text{Be}(d,\alpha_0){}^7\text{Li}$ increases at backward angles, the one of ${}^9\text{Be}(d,\alpha_1){}^7\text{Li}^*$ show opposite tendency (forward high).

The angular distributions of all differential cross sections show asymmetric around 90 degree (both for forward- or backward- peaking). The Oppenheimer-Phillips process (charge polarization) may be considered to explain the asymmetry. However up to now, we can not full-theoretically explain the mechanism of the asymmetry of angular distributions at low energy. To clarify this phenomena, theoretical approaches using on the theory of Distorted Wave Born Approximation (DWBA) processes, Coupled Channel (CC) considering α -cluster model⁽⁷⁾, or R-Matrix theory for the stripping, α -emission, and/or pick-up processes seems to be required.

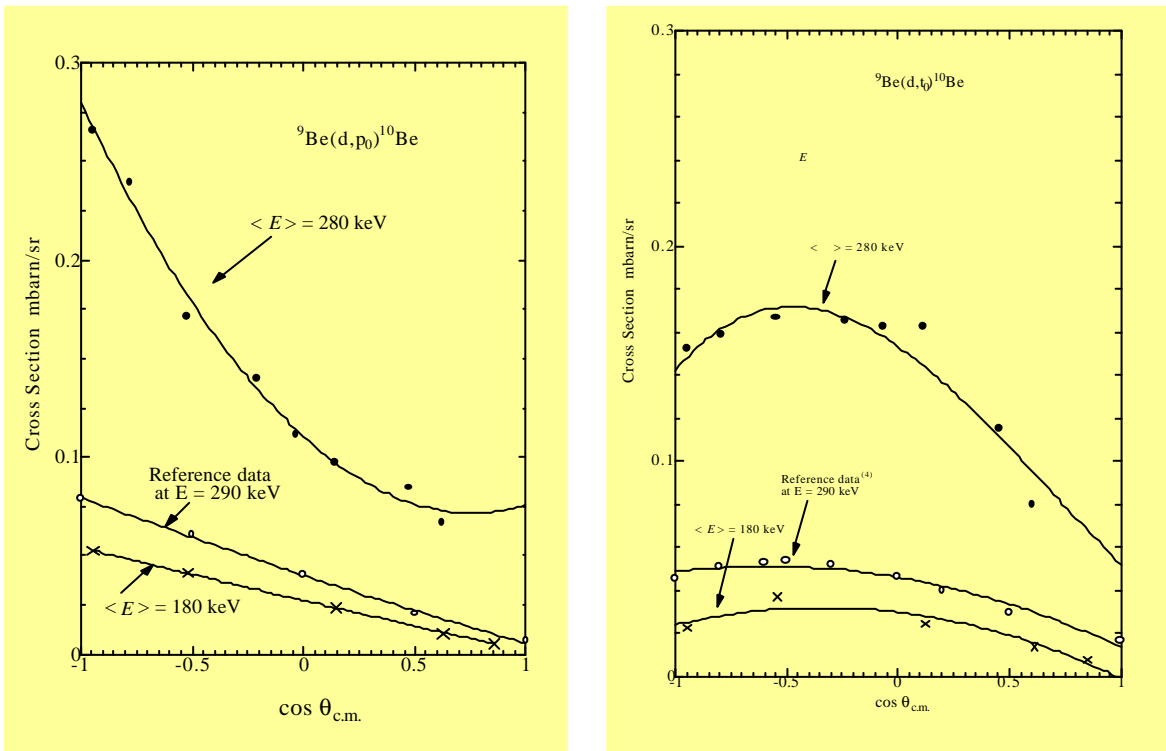


Figure 5 and 6 The angular distributions for ${}^9\text{Be}(d,p)$ and ${}^9\text{Be}(d,t_0)$. at $E = 280$ keV and 180 keV

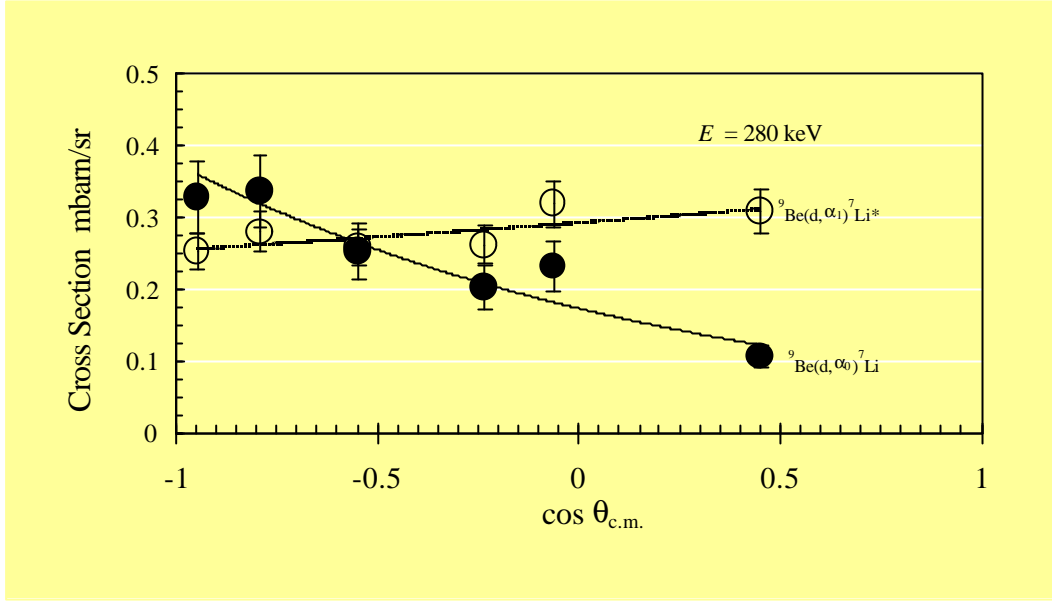


Figure 7 The angular distributions of differential cross sections of ${}^9\text{Be}(d, \alpha_0){}^7\text{Li}$ and ${}^9\text{Be}(d, \alpha_1){}^7\text{Li}^*$ at $E = 280$ keV

The energy dependencies of the cross section for ${}^9\text{Be}(d, p_0){}^{10}\text{Be}$ nuclear reaction, as the representative data, are shown in Fig. 8. All of the measured cross section is the order of μbarns at $E \sim 100$ keV and then cross sections of ${}^9\text{Be}-d$ increase to the order of mbarns at $E \sim 300$ keV. Also, all cross section shows to keep the order of 10 mbarns above $E \sim 0.8$ MeV. Closed triangles in Fig. 8 shows the cross sections obtained from one point experiment (e.g. $4\pi\sigma_{(\theta_r = 90\text{deg.})}$ at $E_{\text{lab.}} = 90\text{-}280$ keV).

Nuclear reaction cross sections ($\sigma_{(E)}$) which drop steeply according to energies E at low energy are given as

$$S_{(E)} = f_{(E)} \cdot S_{(E)} E^{-1} \exp(-2ph) \quad (6)$$

$$f_{(E)} = S_{s(E)} / S_{b(E)} \approx \exp(phU_e / E) \quad (7)$$

where $2\pi\eta = 31.29Z_1Z_2(m/E)^{1/2}$ is the Sommerfeld parameter (Z_1 and $Z_2 =$ charge numbers of interacting nuclei, $m =$ reduced mass in amu, $E =$ c.m. effective incident energy in keV). Also $f_{(E)} = \sigma_{s(E)} / \sigma_{b(E)}$ is the enhancement ratio of the bare cross section ($\sigma_{b(E)}$) and the cross section $\sigma_{s(E)}$ with an electron screening effect in solid target, where U_e is the electron screening potential energy (e.g. $U_e \sim Z_1Z_2 e^2 / r_a$ approximation, with r_a an atomic radius (about $2\text{-}3 \times 10^{-8}$ cm))⁸⁻⁹.

Table 1 shows astrophysical $S_{(E)}$ -factors obtained from the measured cross sections of ${}^9\text{Be}(d, p)$, ${}^9\text{Be}(d, t_0)$, ${}^9\text{Be}(d, \alpha_0)$ and ${}^9\text{Be}(d, \alpha_1)$ at $E_{\text{lab.}} = 90\text{-}280$ keV, respectively. Measured S-factors slightly decrease according as E decreases. However, all of the S-factors at $E = 90$ keV enhanced about twice larger than the one at $E = 140$ keV. For this phenomenon, we assumed that it is not due to the ${}^9\text{Be}-d$ resonance reaction

because excited levels of $^{11}\text{B}^*$ which make S-factor of $^9\text{Be-d}$ reactions enhanced have not found.

We rather suggest that S-factors increase due to an effect of effective electron screening potential (e.g. U_e of formula (7)). The U_e is usually regarded as negligible small value (the order of eV). Therefore, such an enhancement of S-factor appeared hardly at the several hundred keV energy region. However, a recent review paper has reported that the experimental value of the U_e makes the enhancement of S-factors appeared at near $E = 100$ keV⁽¹²⁾. The U_e which was estimated from our S-factors corresponds to the order of 100 eV.

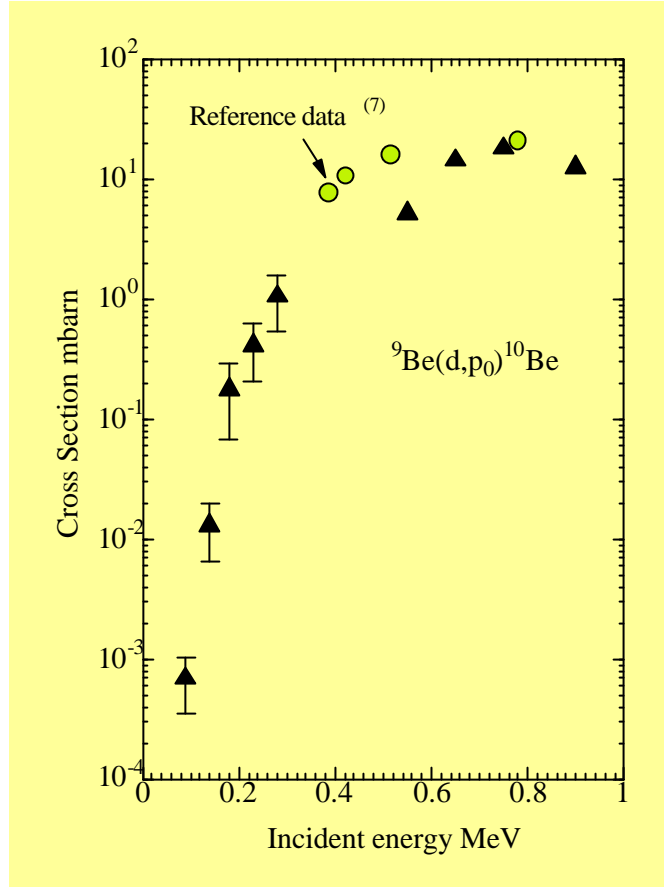


Figure 8 The energy dependencies of the cross section for $^9\text{Be(d,p}_0)^{10}\text{Be}$ nuclear reactions

$\langle E \rangle_{\text{lab}}$ keV	S-factor			
	MeV barn			
	$^9\text{Be(d,}\alpha_0)^7\text{Li}$	$^9\text{Be(d,}\alpha_1)^7\text{Li}^*$	$^9\text{Be(d,p}_0)^{10}\text{Be}$	$^9\text{Be(d,t)}^8\text{Be}$
90	3.5 ± 0.7	5.7 ± 1.2	2.0 ± 0.4	0.9 ± 0.2
140	1.9 ± 0.4	3.1 ± 1.1	1.4 ± 0.3	0.4 ± 0.1
190	2.7 ± 0.6	4.2 ± 0.8	1.7 ± 0.4	0.5 ± 0.1
240	4.3 ± 0.9	6.5 ± 1.3	2.6 ± 0.5	0.9 ± 0.2
290	5.7 ± 1.2	7.6 ± 1.5	2.8 ± 0.6	1.0 ± 0.2

Table 1 Astrophysical $S_{(E)}$ -factors obtained from the measured cross sections of $^9\text{Be(d,p)}$, $^9\text{Be(d,t}_0)$, $^9\text{Be(d,}\alpha_0)$ and $^9\text{Be(d,}\alpha_1)$